

Enhancing Graph Attention Neural Network Performance for Marijuana Consumption Classification through Large-scale Augmented Granger Causality (lsAGC) Analysis of Functional MR Images

Ali Vosoughi^a, Akhil Kasturi^a, and Axel Wismu^{ller}^{a,b,c,d}

^aDepartment of Electrical and Computer Engineering, University of Rochester, NY, USA

^bDepartment of Imaging Sciences, University of Rochester, NY, USA ^cDepartment of Biomedical Engineering, University of Rochester, NY, USA ^dFaculty of Medicine and Institute of Clinical Radiology, Ludwig Maximilian University, Munich, Germany

ABSTRACT

In the present research, the effectiveness of large-scale Augmented Granger Causality (lsAGC) as a tool for gauging brain network connectivity was examined to differentiate between marijuana users and typical controls by utilizing resting-state functional Magnetic Resonance Imaging (fMRI). The relationship between marijuana consumption and alterations in brain network connectivity is a recognized fact in scientific literature. This study probes how lsAGC can accurately discern these changes. The technique used integrates dimension reduction with the augmentation of source time-series in a model that predicts time-series, which helps in estimating the directed causal relationships among fMRI time-series. As a multivariate approach, lsAGC uncovers the connection of the inherent dynamic system while considering all other time-series. A dataset of 60 adults with an ADHD diagnosis during childhood, drawn from the Addiction Connectome Preprocessed Initiative (ACPI), was used in the study. The brain connections assessed by lsAGC were utilized as classification attributes. A Graph Attention Neural Network (GAT) was chosen to carry out the classification task, particularly for its

ability to harness graph-based data and recognize intricate interactions between brain regions, making it appropriate for fMRI-based brain connectivity data. The performance was analyzed using a five-fold cross-validation system. The average accuracy achieved by the correlation coefficient method was roughly 52.98%, with a 1.65 standard deviation, whereas the lsAGC approach yielded an average accuracy of 61.47%, with a standard deviation of 1.44. A random guess method yielded an average accuracy of about 47.05%, with a standard deviation of around 6.25. The study indicates that lsAGC, when paired with a Graph Attention Neural Network, has the potential to serve as a novel biomarker for pinpointing marijuana users, offering a superior and consistent classification strategy over traditional functional connectivity techniques, including the random guess method. The suggested method enhances the body of knowledge in the field of neuroimaging-based classification and emphasizes the necessity to consider directed causal connections in brain network connectivity analysis when studying marijuana's effects on the brain.

Keywords: Graph attention networks (GAT), resting-state fMRI, Large-Scale Augmented Granger Causality, functional connectivity, machine learning, Attention Deficit Hyperactivity Disorder (ADHD), effect of marijuana use

1 INTRODUCTION

Marijuana's longstanding status as an illegal drug, coupled with the apprehensions regarding its negative influence on brain processes and cognitive abilities, has spurred the quest for precise biomarkers to evaluate its ramifications. Studies involving resting-state functional MRI (rs-fMRI) have unveiled that consistent marijuana consumption may modify the brain's connectivity [1,2]. Techniques known as Multi-Voxel Pattern Analysis (MVPA) have been utilized to derive biomarkers from rs-fMRI data, which helps in distinguishing the connectivity patterns between individuals with neurological complications and healthy subjects [1,3].

Most MVPA studies have historically leveraged cross-correlation to assemble a functional connectivity profile, offering optimistic results in terms of information differentiation extracted from fMRI data. However, this method does not encompass directed connectivity, and thus, vital information

in the fMRI data might be overlooked. In our research, we tackle this issue by presenting large-scale Augmented Granger Causality (lsAGC) as an innovative technique for estimating the directed causal links within fMRI time-series [4]. lsAGC employs dimension reduction and predictive modeling of time-series to effectively deduce directed causal dependencies in broad scenarios.

We explore whether variations in directed connectivity might function as biomarkers for regular marijuana intake in adults who were diagnosed with ADHD in childhood, and whether these directed evaluations surpass traditional functional connectivity metrics in classifying frequent marijuana users from typical controls. To this end, we incorporate lsAGC within the MVPA framework to infer directed causal connections among fMRI time-series. For enhancing the classification performance, we engage a Graph Attention Neural Network (GAT) [5] for classification, as it excels in processing graph-related data and discerning complex connections between brain areas, rendering it apt for our brain connectivity data obtained from fMRI.

This paper details the outcomes of our classification trials using lsAGC and GAT and juxtaposes them with traditional cross-correlation-centered approaches. Our discoveries underline lsAGC's merit as a pertinent biomarker for frequent marijuana use and accentuate the efficacy of employing GAT in this setting for elevated classification performance.

This work is embedded in our group's endeavor to expedite artificial intelligence in biomedical imaging by means of advanced pattern recognition and machine learning methods for computational radiology and radiomics, *e.g.*, [6-84].

2 DATA

The ACPI dataset's resting-state fMRI scan parameters can be found on the project's website [85]. We utilized preprocessed data from the MTA 1 dataset [85] of the ACPI database. The dataset initially included 126 subjects, consisting of 101 males and 25 females, with ages between 21-27 years. Of these, 86 were diagnosed with ADHD (68%), and 62 of them regularly used marijuana (49%). Preprocessing of the raw 4D rs-fMRI data was performed using a Configurable

Pipeline for the Analysis of Connectomes (C-PAC) [86] and the Advanced Normalization Tools (ANTs) pipeline. This preprocessing involved the removal of the first five fMRI volumes, anatomical registration, tissue segmentation, functional registration in the Montreal Neurological Institute (MNI) space, functional masking, temporal bandpass filtering (0.01 - 0.1 Hz), motion correction, spatial smoothing, and various nuisance corrections [87]. The MODL parcellation, which is a precomputed atlas for regions definition built using a form of online dictionary learning, was used [1]. For our study, we utilized a subset of the dataset, consisting of 60 subjects, with 32 healthy individuals and 28 diagnosed with marijuana consumption.

Table 1: Distribution of subjects in the subset dataset are listed in this table.

Subject Group	Total Subjects	Marijuana Users
Healthy Controls	32	No
Marijuana Users	28	Yes

3 METHODS

3.1 Large-scale Augmented Granger Causality (lsAGC)

Large-scale Augmented Granger Causality (lsAGC) has been developed based on 1) the principle of original Granger causality, which quantifies the causal influence of time-series \mathbf{x}_s on time-series \mathbf{x}_t by quantifying the amount of improvement in the prediction of \mathbf{x}_t in presence of \mathbf{x}_s . 2) the idea of dimension reduction, which resolves the problem of the tackling a under-determined system, which is frequently faced in fMRI analysis, since the number of acquired temporal samples usually is not sufficient for estimating the model parameters [88].

Consider the ensemble of time-series $X \in \mathbb{R}^{N \times T}$, where N is the number of time-series (Regions Of Interest - ROIs) and T the number of temporal samples. Let $X = (\mathbf{x}_1, \mathbf{x}_2, \dots, \mathbf{x}_N)^\top$ be the whole multidimensional system and $x_i \in \mathbb{R}^{1 \times T}$ a single time-series with $i = 1, 2, \dots, N$, where $\mathbf{x}_i = (x_i(1), x_i(2), \dots, x_i(T))$. In order to overcome the under-determined problem, first X will be decomposed

into its first p high-variance principal components $Z \in \mathbb{R}^{p \times T}$ using Principal Component Analysis (PCA), i.e.,

$$Z = WX, \quad (1)$$

where $W \in \mathbb{R}^{p \times N}$ represents the PCA coefficient matrix. Subsequently, the dimension-reduced time-series ensemble Z is augmented by one original time-series \mathbf{x}_s yielding a dimension-reduced augmented time-series ensemble $Y \in \mathbb{R}^{(p+1) \times T}$ for estimating the influence of \mathbf{x}_s on all other time-series.

Following this, we locally predict the dimension-reduced representation Z of the original highdimensional system X at each time sample t , i.e. $Z(t) \in \mathbb{R}^{p \times 1}$ by calculating an estimate $\hat{Z}_{\mathbf{x}_s}(t)$. To this end, we fit an affine model based on a vector of m vector of m time samples of $Y(\tau) \in \mathbb{R}^{(p+1) \times 1}$ ($\tau = t - 1, t - 2, \dots, t - m$), which is $\mathbf{y}(t) \in \mathbb{R}^{m \cdot (p+1) \times 1}$, and a parameter matrix $A \in \mathbb{R}^{p \times m \cdot (p+1)}$ and a constant bias vector $\mathbf{b} \in \mathbb{R}^{p \times 1}$,

$$\hat{Z}_{\mathbf{x}_s}(t) = A\mathbf{y}(t) + \mathbf{b}, \quad t = m + 1, m + 2, \dots, T. \quad (2)$$

Subsequently, we use the prediction $\hat{Z}_{\mathbf{x}_s}(t)$ to calculate an estimate of X at time t , i.e. $X(t) \in \mathbb{R}^{N \times 1}$ by inverting the PCA of equation (2), i.e.

$$X = W^\dagger Z, \quad (3)$$

where $W^\dagger \in \mathbb{R}^{N \times p}$ represents the inverse of the PCA coefficient matrix W , which is calculated as the *Moore Penrose* pseudoinverse of W . Now $\hat{X}_{\setminus \mathbf{x}_s}(t)$, which is the prediction of $X(t)$ without the information of \mathbf{x}_s , will be estimated. The estimation process is identical to the previous one, with the

only difference being that we have to remove the augmented time-series \mathbf{x}_s and its corresponding column in the PCA coefficient matrix W .

The computation of a lsAGC index is based on comparing the variance of the prediction errors obtained with and without consideration of \mathbf{x}_s . The lsAGC index $f_{\mathbf{x}_s \rightarrow -\mathbf{x}_t}$, which indicates the influence of \mathbf{x}_s on \mathbf{x}_t , can be calculated by the following equation:

$$f_{\mathbf{x}_s \rightarrow -\mathbf{x}_t} = \log \frac{\text{var}(e_s)}{\text{var}(e_{\setminus s})}, \quad (4)$$

where $e_{\setminus s}$ is the error in predicting \mathbf{x}_t when \mathbf{x}_s was not considered, and e_s is the error, when \mathbf{x}_s was used.

3.2 Graph Attention Network (GAT)

Graph Attention Networks (GATs) have emerged as a vital advancement in graph-based deep learning [5], marking a significant departure from conventional Graph Convolutional Networks (GCNs) [89]. Where traditional GCNs treat all neighboring nodes equally, GATs utilize attention mechanisms to assign different importance levels to different nodes, enabling the capture of more complex patterns in data. This attribute is crucial in recognizing and modeling intricate relationships in graph-structured data, an aspect that conventional models often fall short of.

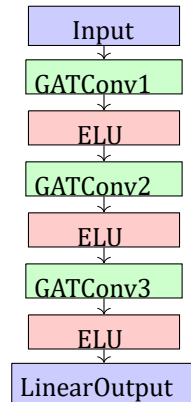


Figure 1: Architecture of the proposed lsAGC + GAT model for classification based on the concept of Granger causality and graph attention neural networks. In this figure, we demonstrate how the GAT model successively refines the graph's representation. Beginning with the initial feature transformation and followed by multiple attention-guided convolutions and ELU activations, the model captures the intricate structure and relationships encoded within the adjacency matrix. The final linear transformation delivers the predictions, effectively leveraging the graph's topology to

inform the underlying task. This layer-by-layer breakdown illustrates the coherent integration of the graph’s structure and node features, achieved through the thoughtful design of the GAT architecture.

Combination of lsAGC and GATs offer an elegant and robust means to model complex relationships in graph-structured data, surpassing traditional methods in both flexibility and expressive power. The architecture of the pipeline of the lsAGC + GAT model is depicted in Figure 1. In the following subsections we detail the method.

3.2.1 Adjacency Matrix

Given a directed graph $G = (V, E)$ with N nodes, the adjacency matrix $\mathbf{F} \in \mathbb{R}^{N \times N}$ is defined such that $F_{ij} = 1$ if there is an edge between nodes i and j , and $F_{ij} = 0$ otherwise. Our method, lsAGC, employs the measure $f_{x_s \rightarrow x_t}$ to determine whether node i (representing x_s) has a causal influence on node j (representing x_t).

3.2.2 Attention Mechanism

Graph Convolutional Networks (GCNs) inherently treat all neighbors equally, often leading to limitations in expressiveness. This poses challenges in the application of GCNs to directional graphs, which are prevalent in our method, the lsAGC. In contrast, Graph Attention Networks (GATs) employ an attention mechanism that emphasizes the more relevant parts of the graph, facilitating a nuanced understanding of the data’s underlying structure.

The attention mechanism in GATs is implemented by calculating attention scores between nodes through a series of learnable parameters and non-linear transformations. The attention scores between nodes i and j are computed as follows:

$$e_{ij} = \text{LeakyReLU}(\mathbf{a}^T [\mathbf{W}\mathbf{h}_i \parallel \mathbf{W}\mathbf{h}_j]), \quad (5)$$

$$\alpha_{ij} = \text{softmax}_j(e_{ij}) = \frac{\exp(e_{ij})}{\sum_{k \in \mathcal{N}(i)} \exp(e_{ik})}. \quad (6)$$

Here, \mathbf{h}_i denotes the feature vector of node i , while \mathbf{W} and \mathbf{a} represent the learnable parameters. In our method, the adjacency matrix obtained using lsAGC, $\mathbf{F} = [f_{x_s \rightarrow -x_t}]$, is considered equal to the node features $\mathbf{H} = [\mathbf{h}_i]_{i=1}^N$, with $\mathbf{F} = \mathbf{H}$, signifying that the graph's structure has an immediate impact on the feature representations. The feature matrix $\mathbf{H} \in \mathbb{R}^{N \times d}$ encapsulates the nodes' attributes, where N is the number of nodes, and d is the dimensionality of the feature space.

The GAT operates on these representations to model intricate relationships between nodes. Attention scores are computed based on the adjacency and feature matrices, and are only calculated for connected nodes, i.e., where $F_{ij} = 1$.

3.2.3 Multi-Head Attention and Aggregation

The Graph Attention Networks (GATs) often utilize a multi-head attention mechanism, which applies multiple sets of learnable parameters to capture diverse facets of relationships between nodes. This method enhances stability in learning and enriches the model's expressiveness by integrating information across various attention heads. In our approach, we averaged the outputs from different heads instead of concatenating them, as given by:

$$\mathbf{h}_i = \text{Aggregate}(\alpha_{ij} \cdot \mathbf{W}\mathbf{h}_j), \forall j \in N(i) \quad (7)$$

The proposed model leverages the adjacency matrix to guide attention, focusing on pertinent relationships while considering connected nodes' features.

3.2.4 Loss Function

In our approach, we utilize the Binary Cross-Entropy Loss with Logits (L_{BCE}) as our chosen loss function. This loss function is applied to the outputs of a linear layer, which represents the predicted class logits, and the encoded feature representations. The modified loss function is formulated as follows:

$$L_{\text{loss}} = L_{BCE}(y, \hat{y}) + L_{BCE}(y_{\text{enc}}, y) \quad (8)$$

Here, \hat{y} signifies the predicted class logits stemming from the linear layer, y_{enc} denotes a transformed encoded representation, and y corresponds to the vector containing the target labels. This loss formulation is operationalized during both the training and validation phases. By combining these two components within the loss, we aim to emphasize distinct facets of the learning task. This approach holds potential for heightened performance and improved generalization across the model's predictions.

3.3 Data Augmentation

Data augmentation is essential for enhancing the diversity of training datasets, mitigating overfitting, and improving generalization in deep learning models. In our study, we exploited specific parameters of the lsAGC method, namely the retained components of PCA and the autoregressive model number, to generate diverse adjacency matrices for each dataset. This augmentation strategy was integrated into the training process, markedly increasing the training sample size. We employed a data augmentation factor of 27, expanding an initial dataset of 60 subjects to a total of 1620 samples. This expansion was instrumental in constructing a robust dataset, a critical factor for the effective training of the Graph Attention Network (GAT) model in our research.

4 RESULTS

Mean connectivity matrices that were extracted using lsAGC and cross-correlation, are shown in Fig. 2 for both typical control and frequent marijuana user cohorts. Different patterns are visible to the naked eye for both methods. In the following, we quantitatively investigate the difference between connectivity patterns of the two subject cohorts using an MVPA approach.

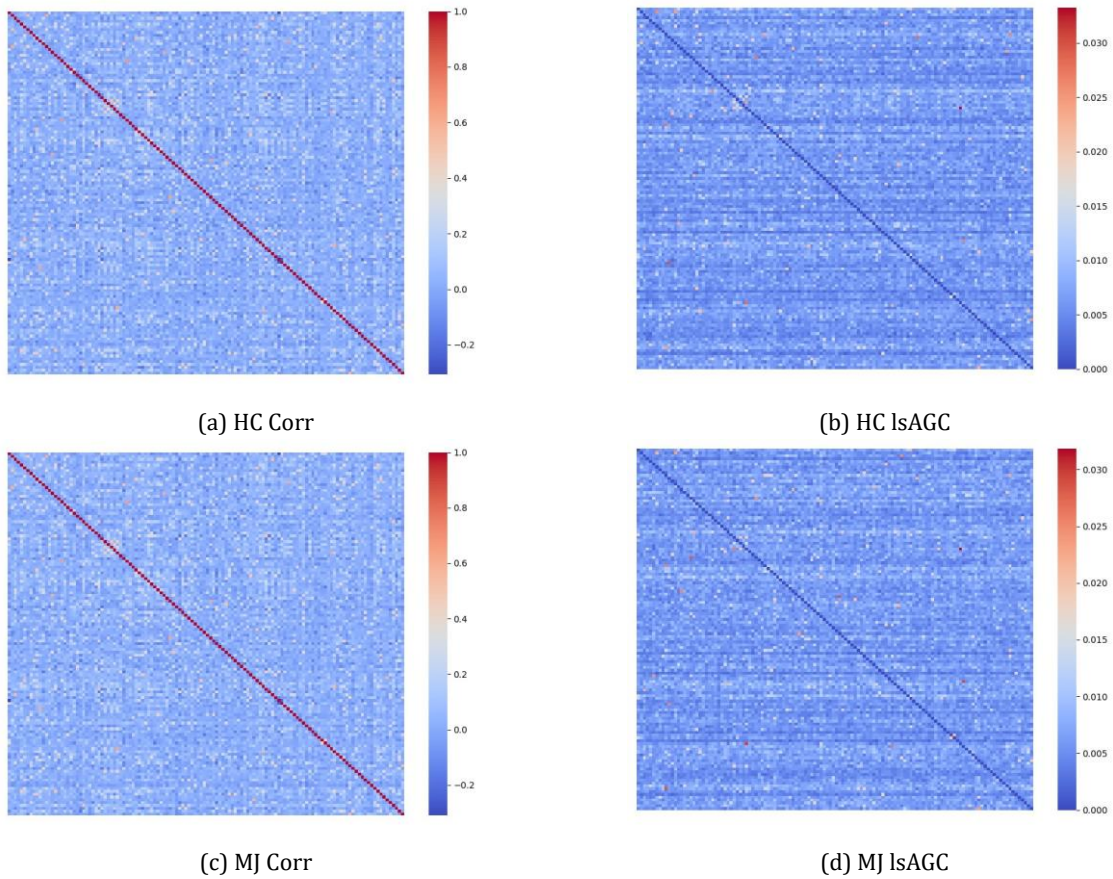


Figure 2: Mean connectivity matrices of control subjects and marijuana users using different methods. Variations in connectivity patterns are observed between the groups.

Table 2: Accuracy Results Comparison for Correlation Coefficient, Random Guess, and Our Method (lsAGC) for five-fold test measures on the dataset.

	lsAGC Accuracy (%)	Correlation Accuracy (%)	Random Guess Accuracy (%)	Std
0	62.28	53.12	46.15	
1	62.53	53.32	56.03	
2	59.73	55.92	45.06	
3	61.65	52.93	48.00	
4	63.18	49.61	40.00	

Mean	61.47	52.98	47.05
Std	1.44	1.65	6.25

The results presented in Table 2 provide insights into the performance of the correlation coefficient method, random guess method, and our method, lsAGC, across five distinct folds. The accuracy values for each method are listed in separate columns, and the results for all three methods are compared across the same five folds.

The mean accuracy computed for the correlation coefficient is approximately 52.98%, while the mean accuracy for our method, lsAGC, is approximately 61.47%. The mean accuracy for random guess method is approximately 47.05%. The standard deviation (Std) for the correlation coefficient method is approximately 1.65, and for the random guess method, it is approximately 6.25. The standard deviation for our method (lsAGC) is approximately 1.44.

These combined results collectively offer valuable insights into the efficacy of the correlation coefficient, random guess, and our method for the specific task. Despite observable performance variance across different folds, the overall performance indicates that our method demonstrates higher accuracy within the experimental setup.

5 CONCLUSIONS

To sum up, the use of large-scale Augmented Granger Causality (lsAGC) as a possible marker to differentiate marijuana users from regular controls is explored in our research by employing restingstate functional Magnetic Resonance Imaging (fMRI). Changes in brain network connectivity connected to marijuana consumption are built upon prior studies, reassessed by probing the ability of lsAGC to effectively distinguish these modifications. The description of directed causal connections within the complex fluctuations of fMRI time-series information is facilitated by lsAGC through a multivariate technique focusing on dimensionality reduction, augmenting data, and time-series predictive modeling. Brain connections are identified using the lsAGC process and used as vital elements for our categorization efforts in a dataset that includes 60 adult subjects who were diagnosed with childhood ADHD from the Addiction Connectome Preprocessed Initiative (ACPI) repository. A

Graph Attention Neural Network (GAT) is used for the categorization task, selected for its competence in handling graph-oriented data and identifying complex connections among various brain areas. Consequently, new possibilities for employing IsAGC-based brain network connectivity to separate marijuana users from standard controls are uncovered by our research, highlighting its potential to enhance our comprehension of the neurological effects tied to marijuana consumption. Further scrutiny and validation through upcoming prospective clinical experiments will be essential to confirm the clinical relevance of our method.

6 Acknowledgements

This research was partially funded by the American College of Radiology (ACR) Innovation Award “AI-PROBE: A Novel Prospective Randomized Clinical Trial Approach for Investigating the Clinical Usefulness of Artificial Intelligence in Radiology” (PI: Axel Wismu“ller) and an Ernest J. Del Monte Institute for Neuroscience Award from the Harry T. Mangurian Jr. Foundation (PI: Axel Wismu“ller). This work was conducted as a Practice Quality Improvement (PQI) project related to the American Board of Radiology (ABR) Maintenance of Certificate (MOC) for A.W.

REFERENCES

- [1] Dadi, K., Rahim, M., Abraham, A., Chyzyk, D., Milham, M., Thirion, B., Varoquaux, G., Initiative, A. D. N., et al., “Benchmarking functional connectome-based predictive models for resting-state fMRI,” *Neuroimage* **192**, 115–134 (2019).
- [2] Solowij, N., [*Cannabis and cognitive functioning*], Cambridge University Press (2006).
- [3] Norman, K. A., Polyn, S. M., Detre, G. J., and Haxby, J. V., “Beyond mind-reading: multivoxel pattern analysis of fMRI data,” *Trends in cognitive sciences* **10**(9), 424–430 (2006).
- [4] Wismu“ller, A. and Vosoughi, M. A., “Large-scale augmented Granger causality (IsAGC) for connectivity analysis in complex systems: From computer simulations to functional MRI (fMRI),” in [*Medical Imaging 2021: Biomedical Applications in Molecular, Structural, and Functional Imaging*], **11600**, 1160009, International Society for Optics and Photonics (2021).
- [5] Casanova, P. V. G. C. A., Lio, A. R. P., and Bengio, Y., “Graph attention networks,” *ICLR. Petar Velickovic Guillem Cucurull Arantxa Casanova Adriana Romero Pietro Li'o and Yoshua Bengio* (2018).
- [6] Bunte, K., Hammer, B., Wismu“ller, A., and Biehl, M., “Adaptive local dissimilarity measures for discriminative dimension reduction of labeled data,” *Neurocomputing* **73**(7-9), 1074–1092 (2010).
- [7] Wismu“ller, A., Vietze, F., and Dersch, D. R., “Segmentation with neural networks,” in [*Handbook of medical imaging*], 107–126, Academic Press, Inc. (2000).

- [8] Wismu"ller, A., Vietze, F., Behrends, J., Meyer-Baese, A., Reiser, M., and Ritter, H., "Fully automated biomedical image segmentation by self-organized model adaptation," *Neural Networks* **17**(8-9), 1327–1344 (2004).
- [9] Hoole, P., Wismu"ller, A., Leinsinger, G., Kroos, C., Geumann, A., and Inoue, M., "Analysis of tongue configuration in multi-speaker, multi-volume MRI data," (2000).
- [10] Wismu"ller, A., "Exploratory morphogenesis (XOM): a novel computational framework for self-organization," *Ph. D. thesis, Technical University of Munich, Department of Electrical and Computer Engineering* (2006).
- [11] Wismu"ller, A., Dersch, D. R., Lipinski, B., Hahn, K., and Auer, D., "A neural network approach to functional MRI pattern analysis—clustering of time-series by hierarchical vector quantization," in [*International Conference on Artificial Neural Networks*], 857–862, Springer (1998).
- [12] Wismu"ller, A., Vietze, F., Dersch, D. R., Behrends, J., Hahn, K., and Ritter, H., "The deformable feature map—a novel neurocomputing algorithm for adaptive plasticity in pattern analysis," *Neurocomputing* **48**(1-4), 107–139 (2002).
- [13] Behrends, J., Hoole, P., Leinsinger, G. L., Tillmann, H. G., Hahn, K., Reiser, M., and Wismu"ller, A., "A segmentation and analysis method for MRI data of the human vocal tract," in [*Bildverarbeitung fu"r die Medizin 2003*], 186–190, Springer (2003).
- [14] Wismu"ller, A., "Neural network computation in biomedical research: chances for conceptual cross-fertilization," *Theory in Biosciences* (1997).
- [15] Bunte, K., Hammer, B., Villmann, T., Biehl, M., and Wismu"ller, A., "Exploratory observation machine (XOM) with Kullback-Leibler divergence for dimensionality reduction and visualization.," in [*ESANN*], **10**, 87–92 (2010).
- [16] Wismu"ller, A., Vietze, F., Dersch, D. R., Hahn, K., and Ritter, H., "The deformable feature map—adaptive plasticity for function approximation," in [*International Conference on Artificial Neural Networks*], 123–128, Springer (1998).
- [17] Wismu"ller, A., "The exploration machine—a novel method for data visualization," in [*International Workshop on Self-Organizing Maps*], 344–352, Springer (2009).
- [18] Huber, M. B., Nagarajan, M., Leinsinger, G., Ray, L. A., and Wismu"ller, A., "Classification of interstitial lung disease patterns with topological texture features," in [*Medical Imaging 2010: Computer-Aided Diagnosis*], **7624**, 762410, International Society for Optics and Photonics (2010).
- [19] Wismu"ller, A., "The exploration machine: a novel method for analyzing high-dimensional data in computer-aided diagnosis," in [*Medical Imaging 2009: Computer-Aided Diagnosis*], **7260**, 72600G, International Society for Optics and Photonics (2009).
- [20] Bunte, K., Hammer, B., Villmann, T., Biehl, M., and Wismu"ller, A., "Neighbor embedding XOM for dimension reduction and visualization," *Neurocomputing* **74**(9), 1340–1350 (2011).
- [21] Meyer-B"ase, A., Lange, O., Wismu"ller, A., and Ritter, H., "Model-free functional MRI analysis using topographic independent component analysis," *International journal of neural systems* **14**(04), 217–228 (2004).
- [22] Wismu"ller, A., "Exploration-organized morphogenesis (XOM): A general framework for learning by self-organization," *Forschungsberichte-Institut fu"r Phonetik und Sprachliche Kommunikation der Universit"at Mu"nchen* (37), 205–239 (2001).
- [23] Saalbach, A., Twellmann, T., Nattkemper, T. W., Wismu"ller, A., Ontrup, J., and Ritter, H. J., "A hyperbolic topographic mapping for proximity data.," in [*Artificial Intelligence and Applications*], **2005**, 106–111 (2005).

- [24] Wismu"ller, A., "A computational framework for nonlinear dimensionality reduction and clustering," in [*International Workshop on Self-Organizing Maps*], 334–343, Springer (2009).
- [25] Leinsinger, G., Teipel, S., Wismu"ller, A., Born, C., Meindl, T., Flatz, W., Sch"onberg, S., Pruessner, J., Hampel, H., and Reiser, M., "Volumetric MRI for evaluation of regional pattern and progressin of neocortical degeneration in alzheimer's disease," *Der Radiologe* **43**(7), 537– 542 (2003).
- [26] Meyer-Base, A., Auer, D., and Wismu"ller, A., "Topographic independent component analysis for fMRI signal detection," in [*Proceedings of the International Joint Conference on Neural Networks, 2003.*], **1**, 601–605, IEEE (2003).
- [27] Wismu"ller, A., "The exploration machine-a novel method for structure-preserving dimensionality reduction.," in [*ESANN*], Citeseer (2009).
- [28] Wismu"ller, A., Lange, O., Auer, D., and Leinsinger, G., "Model-free functional MRI analysis for detecting low-frequency functional connectivity in the human brain," in [*Medical Imaging 2010: Computer-Aided Diagnosis*], **7624**, 76241M, International Society for Optics and Photonics (2010).
- [29] Meyer-Baese, A., Schlossbauer, T., Lange, O., and Wismu"ller, A., "Small lesions evaluation based on unsupervised cluster analysis of signal-intensity time courses in dynamic breast MRI," *International journal of biomedical imaging* **2009** (2009).
- [30] Meyer-B"ase, A., Saalbach, A., Lange, O., and Wismu"ller, A., "Unsupervised clustering of fMRI and MRI time series," *Biomedical Signal Processing and Control* **2**(4), 295–310 (2007).
- [31] Wismu"ller, A., Verleysen, M., Aupetit, M., and Lee, J. A., "Recent advances in nonlinear dimensionality reduction, manifold and topological learning.," in [*ESANN*], (2010).
- [32] Meyer-Baese, A., Lange, O., Wismu"ller, A., and Hurdal, M. K., "Analysis of dynamic susceptibility contrast MRI time series based on unsupervised clustering methods," *IEEE Transactions on Information Technology in Biomedicine* **11**(5), 563–573 (2007).
- [33] Wismu"ller, A., Vietze, F., Dersch, D. R., Hahn, K., and Ritter, H. J., "A neural network approach to adaptive pattern analysis-the deformable feature map.," in [*ESANN*], 189–194 (2000).
- [34] Wismu"ller, A., Behrends, J., Hoole, P., Leinsinger, G. L., Reiser, M. F., and Westesson, P.L., "Human vocal tract analysis by in vivo 3d MRI during phonation: a complete system for imaging, quantitative modeling, and speech synthesis," in [*International Conference on Medical Image Computing and Computer-Assisted Intervention*], 306–312, Springer (2008).
- [35] Wismu"ller, A., Dersch, D. R., Lipinski, B., Hahn, K., and Auer, D., "Hierarchical clustering of functional MRI time-series by deterministic annealing," in [*International Symposium on Medical Data Analysis*], 49–54, Springer (2000).
- [36] Wismu"ller, A., "Method and device for representing multichannel image data," (Nov. 17 2015). US Patent 9,189,846.
- [37] Huber, M. B., Bunte, K., Nagarajan, M. B., Biehl, M., Ray, L. A., and Wismu"ller, A., "Texture feature ranking with relevance learning to classify interstitial lung disease patterns," *Artificial intelligence in medicine* **56**(2), 91–97 (2012).
- [38] Wismu"ller, A., Meyer-Baese, A., Lange, O., Reiser, M. F., and Leinsinger, G., "Cluster analysis of dynamic cerebral contrast-enhanced perfusion MRI time-series," *IEEE transactions on medical imaging* **25**(1), 62–73 (2005).
- [39] Twellmann, T., Saalbach, A., Muller, C., Nattkemper, T. W., and Wismu"ller, A., "Detection of suspicious lesions in dynamic contrast enhanced MRI data," in [*The 26th Annual International Conference of the IEEE Engineering in Medicine and Biology Society*], **1**, 454–457, IEEE (2004).

- [40] Otto, T. D., Meyer-Baese, A., Hurdal, M., Sumners, D., Auer, D., and Wismu"ller, A., "Model-free functional MRI analysis using cluster-based methods," in [*Intelligent Computing: Theory and Applications*], **5103**, 17–24, International Society for Optics and Photonics (2003).
- [41] Varini, C., Nattkemper, T. W., Degenhard, A., and Wismu"ller, A., "Breast MRI data analysis by lle," in [*2004 IEEE International Joint Conference on Neural Networks (IEEE Cat. No. 04CH37541)*], **3**, 2449–2454, IEEE (2004).
- [42] Meyer-Baese, A., Lange, O., Wismuller, A., and Leinsinger, G., "Computer-aided diagnosis in breast MRI based on ICA and unsupervised clustering techniques," in [*Independent Component Analyses, Wavelets, Unsupervised Smart Sensors, and Neural Networks III*], **5818**, 38–49, International Society for Optics and Photonics (2005).
- [43] Huber, M. B., Lancianese, S. L., Nagarajan, M. B., Ikpot, I. Z., Lerner, A. L., and Wismu"ller, A., "Prediction of biomechanical properties of trabecular bone in mr images with geometric features and support vector regression," *IEEE Transactions on Biomedical Engineering* **58**(6), 1820–1826 (2011).
- [44] Meyer-Base, A., Pilyugin, S. S., and Wismu"ller, A., "Stability analysis of a self-organizing neural network with feedforward and feedback dynamics," in [*2004 IEEE International Joint Conference on Neural Networks (IEEE Cat. No. 04CH37541)*], **2**, 1505–1509, IEEE (2004).
- [45] Wismu"ller, A., Dersch, D., Lipinski, B., Hahn, K., and Auer, D., "Hierarchical clustering of fMRI time-series by deterministic annealing," *Neuroimage* **7**(4), S593 (1998).
- [46] Meyer-Baese, A., Lange, O., Schlossbauer, T., and Wismu"ller, A., "Computer-aided diagnosis and visualization based on clustering and independent component analysis for breast MRI," in [*2008 15th IEEE International Conference on Image Processing*], 3000–3003, IEEE (2008).
- [47] Wismu"ller, A., De, T., Lochmu"ller, E., Eckstein, F., and Nagarajan, M. B., "Introducing anisotropic minkowski functionals and quantitative anisotropy measures for local structure analysis in biomedical imaging," in [*Medical Imaging 2013: Biomedical Applications in Molecular, Structural, and Functional Imaging*], **8672**, 86720I, International Society for Optics and Photonics (2013).
- [48] Bhole, C., Pal, C., Rim, D., and Wismu"ller, A., "3d segmentation of abdominal ct imagery with graphical models, conditional random fields and learning," *Machine vision and applications* **25**(2), 301–325 (2014).
- [49] Nagarajan, M. B., Coan, P., Huber, M. B., Diemoz, P. C., Glaser, C., and Wismu"ller, A., "Computer-aided diagnosis in phase contrast imaging x-ray computed tomography for quantitative characterization of ex vivo human patellar cartilage," *IEEE Transactions on Biomedical Engineering* **60**(10), 2896–2903 (2013).
- [50] Wismu"ller, A., Behrends, J., Dersch, D., Leinsinger, G., Vietze, F., and Hahn, K., "Automatic segmentation of cerebral contours in multispectral MRI data sets of the human brain by selforganizing neural networks," in [*Radiology*], **221**, 461–461 (2001).
- [51] Wismueller, A., Vietze, F., Dersch, D., Leinsinger, G., Ritter, H., and Hahn, K., "Adaptive self-organized template matching of the gray-level feature space for automatic segmentation of multispectral MRI data of the human brain," in [*Radiology*], **213**, 364–364 (1999).
- [52] Meyer-Baese, A., Wismu"ller, A., Lange, O., and Leinsinger, G., "Computer-aided diagnosis in breast MRI based on unsupervised clustering techniques," in [*Intelligent Computing: Theory and Applications II*], **5421**, 29–37, International Society for Optics and Photonics (2004).
- [53] Nagarajan, M. B., Coan, P., Huber, M. B., Diemoz, P. C., Glaser, C., and Wismu"ller, A., "Computer-aided diagnosis for phase-contrast x-ray computed tomography: quantitative characterization of human patellar cartilage with high-dimensional geometric features," *Journal of digital imaging* **27**(1), 98–107 (2014).

- [54] Pester, B., Leistrütz, L., Witte, H., and Wismüller, A., "Exploring effective connectivity by a Granger causality approach with embedded dimension reduction," *Biomedical Engineering/Biomedizinische Technik* **58**(SI-1-Track-G), 000010151520134172 (2013).
- [55] Nagarajan, M. B., Huber, M. B., Schlossbauer, T., Leinsinger, G., Krol, A., and Wismüller, A., "Classification of small lesions on dynamic breast MRI: Integrating dimension reduction and out-of-sample extension into cadx methodology," *Artificial intelligence in medicine* **60**(1), 65–77 (2014).
- [56] Abidin, A. Z., Deng, B., DSouza, A. M., Nagarajan, M. B., Coan, P., and Wismüller, A., "Deep transfer learning for characterizing chondrocyte patterns in phase contrast x-ray computed tomography images of the human patellar cartilage," *Computers in biology and medicine* **95**, 24–33 (2018).
- [57] Chockanathan, U., Abidin, A. Z., DSouza, A. M., Schifitto, G., and Wismüller, A., "Resilient modular small-world directed brain networks in healthy subjects with large-scale Granger causality analysis of resting-state functional MRI," in [*Medical Imaging 2018: Biomedical Applications in Molecular, Structural, and Functional Imaging*], **10578**, 105780B, International Society for Optics and Photonics (2018).
- [58] DSouza, A. M., Abidin, A. Z., Chockanathan, U., Schifitto, G., and Wismüller, A., "Mutual connectivity analysis of resting-state functional MRI data with local models," *NeuroImage* **178**, 210–223 (2018).
- [59] Chockanathan, U., DSouza, A. M., Abidin, A. Z., Schifitto, G., and Wismüller, A., "Automated diagnosis of HIV-associated neurocognitive disorders using large-scale Granger causality analysis of resting-state functional MRI," *Computers in Biology and Medicine* **106**, 24–30 (2019).
- [60] Abidin, A. Z., Dar, I., D'Souza, A. M., Lin, E. P., and Wismüller, A., "Investigating a quantitative radiomics approach for brain tumor classification," in [*Medical Imaging 2019: Biomedical Applications in Molecular, Structural, and Functional Imaging*], **10953**, 109530B, International Society for Optics and Photonics (2019).
- [61] DSouza, A. M., Abidin, A. Z., and Wismüller, A., "Classification of autism spectrum disorder from resting-state fMRI with mutual connectivity analysis," in [*Medical Imaging 2019: Biomedical Applications in Molecular, Structural, and Functional Imaging*], **10953**, 109531D, International Society for Optics and Photonics (2019).
- [62] Abidin, A. Z., DSouza, A. M., Schifitto, G., and Wismüller, A., "Detecting cognitive impairment in HIV-infected individuals using mutual connectivity analysis of resting state functional MRI," *Journal of neurovirology* **26**(2), 188–200 (2020).
- [63] Wismüller, A. and Stockmaster, L., "A prospective randomized clinical trial for measuring radiology study reporting time on artificial intelligence-based detection of intracranial hemorrhage in emergent care head ct," in [*Medical Imaging 2020: Biomedical Applications in Molecular, Structural, and Functional Imaging*], **11317**, 113170M, International Society for Optics and Photonics (2020).
- [64] Wismüller, A., DSouza, A. M., Abidin, A. Z., and Vosoughi, M. A., "Large-scale nonlinear Granger causality: A data-driven, multivariate approach to recovering directed networks from short time-series data," *arXiv preprint arXiv:2009.04681* (2020).
- [65] Vosoughi, A., DSouza, A., Abidin, A., and Wismüller, A., "Relation discovery in nonlinearly related large-scale settings," in [*ICASSP 2022-2022 IEEE International Conference on Acoustics, Speech and Signal Processing (ICASSP)*], 5103–5107, IEEE (2022).
- [66] Vosoughi, M. A. and Wismüller, A., "Large-scale kernelized Granger causality to infer topology of directed graphs with applications to brain networks," *arXiv preprint arXiv:2011.08261* (2020).

- [67] Vosoughi, M. A. and Wismu"ller, A., "Large-scale extended granger causality for classification of marijuana users from functional mri," in [*Medical Imaging 2021: Biomedical Applications in Molecular, Structural, and Functional Imaging*], **11600**, 116000D, International Society for Optics and Photonics (2021).
- [68] Wismu"ller, A. and Vosoughi, M. A., "Classification of schizophrenia from functional MRI using large-scale extended Granger causality," *International Society for Optics and Photonics* (2021).
- [69] Wismu"ller, A., Dsouza, A. M., Vosoughi, M. A., and Abidin, A., "Large-scale nonlinear Granger causality for inferring directed dependence from short multivariate time-series data," *Scientific reports* **11**(1), 1–11 (2021).
- [70] Vosoughi, M. A. and Wismu"ller, A., "Leveraging pre-images to discover nonlinear relationships in multivariate environments," in [*2021 European Signal Processing Conference (EUSIPCO)*], IEEE (August 2021).
- [71] Vosoughi, M. A. and Wismu"ller, A., "Large-scale kernelized granger causality (lskgc) for inferring topology of directed graphs in brain networks," in [*Medical Imaging 2022: Biomedical Applications in Molecular, Structural, and Functional Imaging*], **12036**, 1203603, SPIE (2022).
- [72] Hadjiyski, N., Kasturi, A., Vosoughi, A., and Wismu"ller, A., "Leveraging a memory-driven transformer for efficient radiology report generation from chest x-rays to establish a quantitative metric," in [*Emerging Topics in Artificial Intelligence (ETAI) 2024*], **13118**, 10–22, SPIE (2024).
- [73] Kasturi, A., Vosoughi, A., Hadjiyski, N., Stockmaster, L., and Wismu"ller, A., "Functional connectivity-based classification of autism spectrum disorder using mutual connectivity analysis with local models," in [*Emerging Topics in Artificial Intelligence (ETAI) 2024*], **13118**, 23–31, SPIE (2024).
- [74] Kasturi, A., Vosoughi, A., Hadjiyski, N., Stockmaster, L., Sehnert, W. J., and Wismu"ller, A., "Anatomical landmark detection in chest x-ray images using transformer-based networks," in [*Medical Imaging 2024: Computer-Aided Diagnosis*], **12927**, 647–660, SPIE (2024).
- [75] Kasturi, A., Vosoughi, A., Hadjiyski, N., Stockmaster, L., Sehnert, W. J., and Wismu"ller, A., "Classification of endotracheal tube position in chest x-rays images," in [*Medical Imaging 2024: Clinical and Biomedical Imaging*], **12930**, 142–153, SPIE (2024).
- [76] Vosoughi, A., Kasturi, A., and Wismu"ller, A., "Enhancing graph attention neural network performance for marijuana consumption classification through large-scale augmented granger causality (lsagc) analysis of functional mr images," in [*Medical Imaging 2024: Clinical and Biomedical Imaging*], **12930**, 172–189, SPIE (2024).
- [77] Kasturi, A., Vosoughi, A., Hadjiyski, N., Stockmaster, L., Sehnert, W. J., and Wismu"ller, A., "Segmentation of catheter tubes and lines in chest x-rays using deep learning models," in [*Medical Imaging 2024: Clinical and Biomedical Imaging*], **12930**, 112–125, SPIE (2024).
- [78] Vosoughi, A., Kasturi, A., and Wismu"ller, A., "Graph attention transformers and large-scale granger causality to classify marijuana consumption from functional mr images," in [*Medical Imaging 2024: Clinical and Biomedical Imaging*], **12930**, 283–299, SPIE (2024).
- [79] Kasturi, A., Vosoughi, A., Hadjiyski, N., Stockmaster, L., Sehnert, W. J., and Wismu"ller, A., "Detecting landmarks in anatomical medical images using transformer-based networks," in [*Emerging Topics in Artificial Intelligence (ETAI) 2023*], **12655**, 46–56, SPIE (2023).
- [80] Vosoughi, A., Raiser, T., Luther, T., Willacker, L., Rosenfelder, M., Kasturi, A., Sitt, J. D., Manasova, D., Comanducci, A., Bender, A., et al., "Leveraging large-scale granger causality and neural networks to measure the level of consciousness in doc patients," in [*Emerging Topics in Artificial Intelligence (ETAI) 2023*], **12655**, 32–45, SPIE (2023).

- [81] Wismu"ller, A., Vosoughi, A., Kasturi, A., and Hadjiyski, N., "Identification of schizophrenia patients using large-scale extended granger causality (lsxgc) in functional mr imaging," in [*Medical Imaging 2023: Biomedical Applications in Molecular, Structural, and Functional Imaging*], **12468**, 269–277, SPIE (2023).
- [82] Wismu"ller, A., Vosoughi, A., Kasturi, A., and Hadjiyski, N., "Large-scale granger causality (lsgc) for classification of schizophrenia using functional mri," in [*Medical Imaging 2023: Biomedical Applications in Molecular, Structural, and Functional Imaging*], **12468**, 287–295, SPIE (2023).
- [83] Wismu"ller, A., Vosoughi, A., Kasturi, A., and Hadjiyski, N., "Large-scale augmented granger causality (lsagc) for discovery of causal brain connectivity networks in schizophrenia patients using functional mri neuroimaging," in [*Medical Imaging 2023: Biomedical Applications in Molecular, Structural, and Functional Imaging*], **12468**, 278–286, SPIE (2023).
- [84] Vosoughi, A., Kasturi, A., Hadjiyski, N., and Wismu"ller, A., "Classification of schizophrenia using large-scale kernelized granger causality (lskgc) and functional mr imaging," in [*Medical Imaging 2023: Computer-Aided Diagnosis*], **12465**, 35–44, SPIE (2023).
- [85] MTA 1, "<http://fcon.1000.projects.nitrc.org/indi/acpi/html/>," (2015). Last accessed 20 August 2020.
- [86] C-PAC, "<https://fcp-indi.github.io/>," (2015). Last accessed 20 August 2020.
- [87] The INDI Team, "ACPI preprocessing pipelines," (2015). Last accessed 20 August 2020.
- [88] DSouza, A. M., Abidin, A. Z., Leistriz, L., and Wismu"ller, A., "Exploring connectivity with large-scale Granger causality on resting-state functional MRI," *Journal of neuroscience methods* **287**, 68–79 (2017).
- [89] Kipf, T. N. and Welling, M., "Semi-supervised classification with graph convolutional networks," *arXiv preprint arXiv:1609.02907* (2017).